Journal of Nanostructure in Chemistry (2019) 9:247–258
https://doi.org/10.1007/s40097-019-00315-y

ORIGINAL RESEARCH

Fabrication of nanosized SO_4^{2-}/Co–Al mixed oxide via solution combustion method used in esterification reaction: effect of urea-nitrate ratio on the properties and performance

Amir-Hossein Azmoon[1] · Ali Ahmadpour[1] · Hamed Nayebzadeh[2] · Naser Saghatoleslami[1,3] · Alireza Heydari[1]

Received: 9 May 2019 / Accepted: 7 August 2019 / Published online: 17 August 2019

Abstract

Recently, mixed metal aluminate as a highly active, stable, and reusable nanocatalyst was extremely used in chemical reactions such as esterification. The preparation of the samples via a simple, rapid, and cost-effective method is one of the main problems on the front of the industrial application of these materials. For this purpose, the solution combustion method (SCM) was assessed for the fabrication of spinel $CoAl_2O_4$, and the effects of fuel-to-oxidizer (*F*/*O*) ratio on crystalline structure, surface functional groups, surface area, morphology, and porosity were analyzed. The activity of the samples, which was impregnated by the sulfate group was evaluated in the esterification reaction. Morphology and texture properties of the samples indicated the crystallinity, surface area, and pore diameter of $CoAl_2O_4$ were enhanced by increasing the *F*/*O* ratio. It can be related to increasing the combustion reaction time and temperature. However, at *F*/*O* ratios above two, due to limited diffusion of oxygen into the reaction medium, the reaction terminated immaturely. Sulfated cobalt aluminate fabricated at *F*/*O* ratio of two was successfully synthesized in nanoscale with same particle size. Moreover, it did not show impurity in its structure that is related to the ability of the combustion method for the fabrication of pure nanocatalyst. Evaluation of the catalytic activity of the SO_4^{2-}/$CoAl_2O_4$ nanocatalysts in the esterification reaction confirmed the results of physicochemical studies. For instance, the sample prepared at *F*/*O* ratio of two presented the highest conversion (96.7%) at methanol/oleic acid molar ratio of nine, catalyst amount of 3 wt. %, and reaction temperature and time of 120 °C and 4 h, respectively. In addition to preserving its activity for four runs (conversion > 85%), its activity was simply recovered upon regeneration by sulfate group, making it a promising alternative for industrial production of biodiesel.

✉ Hamed Nayebzadeh
h.nayebzadeh@esfarayen.ac.ir

[1] Department of Chemical Engineering, Faculty of Engineering, Ferdowsi University of Mashhad, P.O. Box 9177948974, Mashhad, Iran

[2] Esfarayen University of Technology, Esfarayen, North Khorasan, Iran

[3] Department of Petroleum Engineering, Eqbal Institute of Higher Education, Mashhad, Iran

Graphic abstract

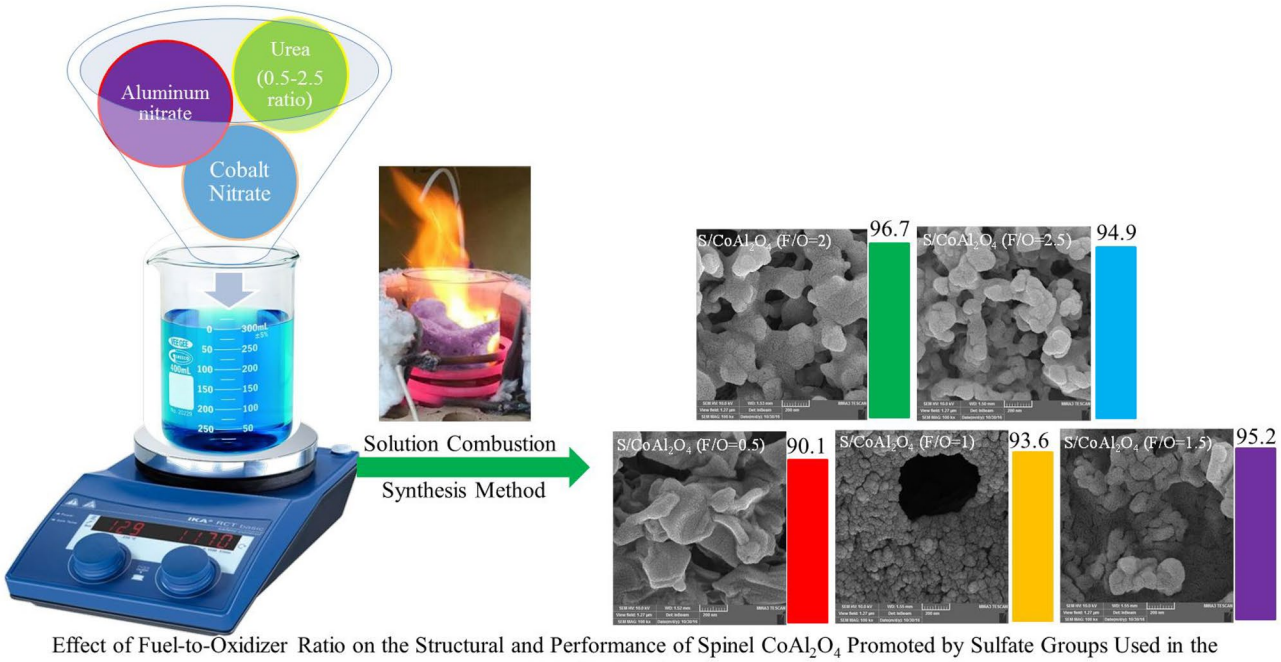

Effect of Fuel-to-Oxidizer Ratio on the Structural and Performance of Spinel $CoAl_2O_4$ Promoted by Sulfate Groups Used in the Esterification Reaction

Keywords Cobalt aluminate · Nanocatalyst · Solution combustion method (SCM) · Fuel to oxidizer ratio · Esterification · Biodiesel

Introduction

Upon increased attention to air pollution and climate changes resulted from hydrocarbon emissions, governors are trying to provide laws for lowering the consumption of petroleum fuels by replacing them with renewable fuels [1]. A green fuel with similar properties to diesel fuel is hugely desired because of producing lower levels of hydrocarbon emissions and reducing the problem of compatibility the green fuel with the diesel engine. Biodiesel (fatty acid alkyl esters) is produced either upon esterification of free fatty acids (FFAs) using acid catalysts or transesterification of triglycerides with base catalysts. Although the transesterification reaction is the general process for conversion of biomass to biodiesel, the sensitivity of this process to the quality of the oil is a limitation. Due to remarkably increasing the biodiesel production cost using crude vegetable oils, low-cost feedstock such as inedible oils, which have high FFA contents, are suggested. However, alkali transesterification reaction cannot utilize due to soap formation by the reaction between FFA and base catalyst. Therefore, the oils contained high amounts of FFAs must react with a short-chain alcohol for reducing their FFA content for biodiesel production in which an acid catalyst is usually used. In this reaction as called esterification reaction, strong mineral acid catalysts such as H_2SO_4, HF, and HNO_3 are generally used [2]. Although a pre-step (esterification) was recommended to decrease the FFA content of oils [3], disadvantages associated with homogeneous acid catalysts, such as corrosion, massive wastewater production during neutralization of final product, and salt generation, have increasingly led researchers toward cleaner technologies, e.g., heterogeneous acid catalysts [2].

Because of their particular advantages, heterogeneous acid catalysts have been significantly evaluated to replace homogeneous acid catalysts [4, 5]. Specially designed heterogeneous catalysts offer high activity and selectivity along with simple recovery from reaction medium without waste production as well as reusability [6, 7]. Aluminosilicate [8], $SO_4^{2-}/La^{3+}/C$ [9], and $ZnAl_2O_4$ [10], respectively, present the ability for using for 3, 10, and 4 times in the reaction. Many solid catalysts with the acidic property have been studied for the esterification of FFAs, such as sulfated metal oxides [11], sulfated carbon [12], ion-exchange resins [13] and acid ionic liquids [14]. Although, the solid acid catalysts have successfully converted a high amount of FFA to ester during esterification reaction,

some reaction conditions were beyond the standard range for the esterification reaction via homogeneous acid catalyst (reaction temperature of 60–120 °C, methanol/FFA molar ratio (MFR) of 6–12, catalyst concentration of 3–10 wt %, and reaction time of 2–4 h). Saravanan et al. [15, 16] used a methanol/FFA molar ratio of 20 at catalyst (sulfated zirconia) concentration of 6 wt % for 7 h of reaction time to obtain a yield of about 90%. Duan et al. [11] performed esterification reaction of octanoic acid at 160 °C using 50 wt % SO_4^{2-}/Al_2O_3–SiO as a catalyst for 3 h and ended up with a yield of 93%. Sulfated Zr-KIT-6 (20) was used for esterification of oleic acid, and a conversion yield of 96% was reached at 120 °C, 4 wt % of catalyst, 20 MFR, 6 h of reaction time [17].

However, leaching the active phases (especially for the catalysts impregnated by sulfate group) and deformation of the support structure (mixed metal oxides) after uses in the reaction are the major drawbacks of some of these catalysts.

Recently, several studies have pointed out high stability and activity of mixed metal aluminate catalysts in esterification and transesterification reactions [18, 19]. Metal ion-doped aluminum provides large surface area and high thermal and mechanical stability as well as chemical resistance, making it promising support [20, 21]. Zinc aluminate and copper aluminate nanocatalysts were one of them that have been evaluated in the esterification of oleic acid [10]. Moreover, the reactions have been improved by the fabrication of a novel $Zn_{1-x}Cu_xAl_2O_4$ nanocatalyst, thereby achieving a yield of as high as 96.9% [22]. SO_3H–$ZnAl_2O_4$ solid acid catalyst was in the esterification reaction, and the highest FAME yield was achieved (94.59%) at 60 °C, 1.5 wt % of catalyst, 9 MFR [23]. Although the properties of $MgO/MgAl_2O_4$ [24] and KOH/calcium aluminate nanocatalysts [25] were thoroughly studied in the transesterification reaction, to the best of our knowledge, no study has been performed on the activity of cobalt aluminate ($CoAl_2O_4$) as support in the esterification reaction.

Solution combustion method (SCM) as one of the effective methods was recently utilized to synthesize powders, extensively [26, 27]. It has been reported that SCM is an appropriate method for fabrication of nanocatalyst via a fast and straightforward synthesis approach that can be a suitable choice for reactions in the liquid medium such as biodiesel production. The nanosized catalyst can purely be synthesized via SCM with appropriate structural, textural properties, and performance [24].

In the present study, cobalt spinel ($CoAl_2O_4$) was synthesized by SCM, and as a critical parameter in SCM, fuel-to-oxidizer (F/O) ratio was optimized based on its influence on the properties and performance of $CoAl_2O_4$ in the esterification reaction. Sulfated $CoAl_2O_4$ nanocatalysts were characterized by X-ray diffraction analysis (XRD), thermogravimetric (TG) studies, Fourier-transform infrared spectroscopy (FTIR), Brunauer–Emmett–Teller and Barrett-Joyner-Halenda (BET–BJH) analysis, field emission scanning electron microscopy (FESEM), and Energy-dispersive X-ray spectroscopy (EDX), and actually examined in the esterification of oleic acid. Finally, the stability of the optimal sulfated cobalt aluminate was evaluated to assess its application for biodiesel production on an industrial scale.

Materials and methods

Catalyst preparation

For the preparation of $SO_4^{2-}/CoAl_2O_4$ as a nanocatalyst, firstly, cobalt spinel ($CoAl_2O_4$) was synthesized as support via solution combustion method. In this method, nitrate type of metal salts are dissolved in distilled water and appropriate amounts of fuel determined according to propellant chemistry, i.e., the ratio of oxidizer to reducer valences of components, was then added. Therefore, 0.02 mol of aluminum nitrate nonahydrate ($Al(NO_3)_3.9H_2O$, 99%, Merck) and 0.01 mol of cobalt nitrate hexahydrate ($Co(NO_3)_2.6H_2O$, 99%, Merck) were mixed into 40 mL of distilled water and then urea (NH_2CONH_2, 99%, Merck) as fuel was added at various stoichiometric ratios (0.5, 1, 1.5, 2 and 2.5). Based on the stoichiometric ratio of urea (6.67 mmol), the reaction equation is presented as follows:

$$\begin{aligned} &Co(NO_3)_2.6H_2O + 2Al\left(NO_3\right)_3.9H_2O \\ &\quad + 6.67Y\ CO\left(NH_2\right)_2 \rightarrow CoAl_2O_4 \\ &\quad + 6.67Y\ CO_2 + (24+13.34Y)\,H_2O \\ &\quad + (4+6.67Y)\,N_2,\ Y = 0.5, 1, 1.5,\ 2 \text{ and } 2.5, \end{aligned} \tag{1}$$

where Y is a proportion of F/O compared to the stoichiometric ratio.

After heating the mixture on a hotplate at 80 °C, excess water was evaporated, and a viscous gel was obtained. The gel was then put into an electric furnace at 350 °C. After evaporation of the residual water of the gel, a white smoke released indicating that the solution has reached the point of spontaneous combustion. Subsequently, an exothermic reaction with visible flame began at auto-ignition temperature. Finally, a low-density foamy solid powder was obtained, which was further crushed in a ceramic mortar and set in a desiccator. Based on the used F/O, the obtained substances were labeled as $CoAl_2O_4$ ($F/O = 0.5$), $CoAl_2O_4$ ($F/O = 1$), $CoAl_2O_4$ ($F/O = 1.5$), $CoAl_2O_4$ ($F/O = 2$) and $CoAl_2O_4$ ($F/O = 2.5$).

In the second step, sulfate groups were loaded on the synthesized supports via impregnation method. For this purpose, 10 mL of an aqueous solution of H_2SO_4 (1 M) was mixed with 1 g of each cobalt spinel ($CoAl_2O_4$) support and

the mixture was stirred for 3 h under reflux at 80 °C. Then, the mixture was placed in an oven at 110 °C for overnight to dry and calcined at 550 °C for 3 h in air ambient. The samples were labeled as S/$CoAl_2O_4$ ($F/O = 0.5$), S/$CoAl_2O_4$ ($F/O = 1$), S/$CoAl_2O_4$ ($F/O = 1.5$), S/$CoAl_2O_4$ ($F/O = 2$) and S/$CoAl_2O_4$ ($F/O = 2.5$).

Catalyst characterization

The XRD was detected using Cu K_α radiation in the range of 10–60° using UNISANTIS/XMD 300 apparatus operating at 45 kV and 80 mA to determine the crystalline phase of the samples. Moreover, the Scherrer equation was utilized for calculating the crystalline size of the samples. The quality of decompositions of presursores during the synthesis of supports via combustion reaction was assessed by TG analysis (Evolution STA, SETARAM, France) in which the temperature was increased from ambient to 900 °C at a heating rate of 20 °C/min. The FTIR for evaluating the active surface functional groups of the nanocatalysts was performed using SHIMADZU 4300 (Japan) spectrometer in the range of 400-4000 cm^{-1}. The textural properties containing the specific surface area, mean pore size and pore volume of the sulfated nanocatalysts along with adsorption–desorption hystersis and pore size distribution plots were measured by BET-BJH method using PHS-1020 (PHSCHINA, China) apparatus. The morphology, particle size, external porosity, and surface structure of the nanocatalysts were studied using FESEM images pictured by MIRA3 FEG-SEM (TESCAN, Czech Republic) instrument. Moreover, the EDX technique using VEGA II Detector (Czech Republic, TESCAN) was utilized for assessing the distribution of elements in the samples. The acid strength of the solid nanocatalyst (H_0) was determined using Hammett indicators. Methyl red ($H_0 = 4.8$), *p*-dimethylaminoazobenzene ($H_0 = +3.3$), violet crystal ($H_0 = 0.8$) and dicinnamalacetone ($H_0 = -3.0$, basic) were utilized as Hammett indicators. The acid strength of samples was determined by the titration method using 0.01 N Butyl-Amin solution [28].

Esterification reaction

The activity of sulfated cobalt spinel nanocatalysts was assessed in the esterification reaction of oleic acid. Because of the high percentage of oleic acid ($C_{18}H_{34}O_2$, 9-octadecenoic acid), as an unsaturated fatty acid, in both edible and non-edible oils, it was selected for the esterification reaction. 20 g of oleic acid, 0.6 g of catalyst (3 wt %), and 25.8 mL of methanol (methanol-to-oleic acid molar ratio of 9) were poured into a 100 ml stainless steel batch reactor equipped with a thermocouple (Type K) and a magnetic stirrer. The esterification reaction was carried out at 90 ± 2 °C and 120 ± 2 °C for 4 h in which the mixture was stirred at constant stirring rate of 600 rpm. Following each run, the reactor was cooled down to room temperature. Once the mixture was settled in a separation funnel, the top layer containing methyl ester (ME) was separated and heated to purify ME from excess methanol and water. Accordingly, the conversion was determined based on reducing the acidity of oleic acid, as measured by standard titration method using 0.1 M alcoholic potassium hydroxide and phenolphthalein, according below equation:

$$\mathrm{AI} = 5.61\, V / W. \tag{2}$$

$$\text{Conversion } (\%) = 100\left(\mathrm{AI}_{\text{Oleic acid}} - \mathrm{AI}_{\mathrm{ME}}\right) / \mathrm{AI}_{\text{oleic acid}}, \tag{3}$$

where AI is acid index, V is the volume of alcoholic potassium hydroxide consumed during titration and W is the weight of ME sample.

Results and discussion

XRD analysis

XRD plots of $CoAl_2O_4$ as support synthesized by SCM at different F/O ratios are illustrated in Fig. 1a. It has been reported that properties of the powder synthesized by SCM such as crystallite phase and size, textural properties, and particle shape and size are generally organized by the F/O ratio [29]. The samples present the spinel structure of $CoAl_2O_4$ (JCPDS No. 3–0896) that its crystallinity increases by more loading urea (i.e., increasing F/O ratio). Although cobalt oxide structures (Co_3O_4, JCPDS No. 80–1535) can observe, these peaks reduce and disappear by increasing the F/O ratio (especially more than 1.5). changes in the peaks could be related to the diffusion of cobalt ions into alumina lattice as a result of increased temperature and duration of combustion reaction [27, 30].

However, the cobalt oxide structure was observed at F/O ratio of 2.5. Indeed, rapid oxygen diffusion from the air is a requirement for complete combustion in fuel-rich condition [31]. However, the combustion reaction terminated immaturely because of limited diffusion of oxygen from the air into the reaction medium as a result the huge volume of smoke released from the reaction medium [32]. Therefore, the diffusion of Co ions into alumina lattice was not occurred.

Figure 1b shows XRD patterns of the sulfated cobalt aluminate. The cobalt sulfate ($CoSO_4$, JCPDS No. 72–1455) and aluminate sulfate ($Al_2(SO_4)_3$, JCPDS No. 80–1535) structures formed on the cobalt aluminate. Well-bonding of sulfate groups with the surface of support fabricated at higher F/O ratio (over 1.5) can be related to higher

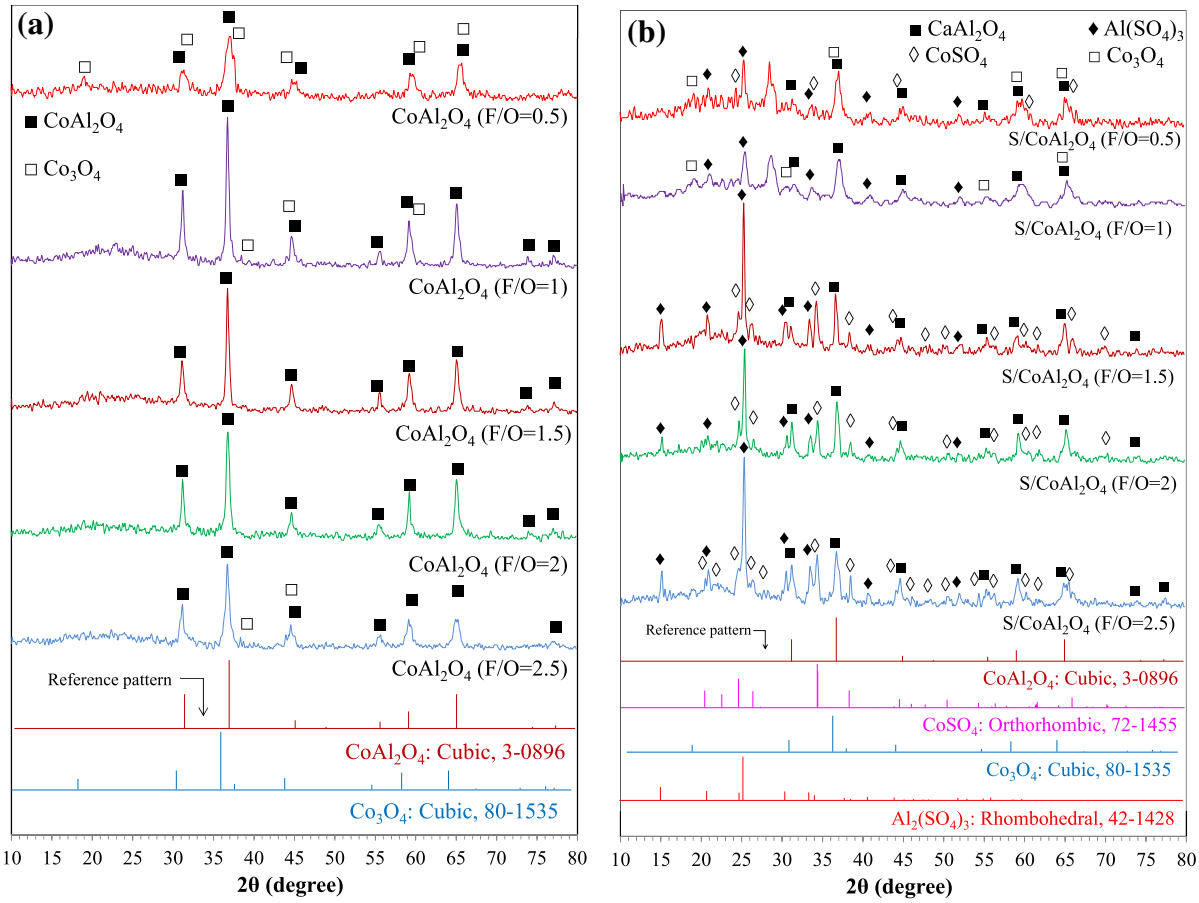

Fig. 1 XRD patterns of **a** $CoAl_2O_4$ and **b** sulfated $CoAl_2O_4$ prepared via solution combustion method at different *F/O*

Table 1 Physicochemical properties of the samples prepared via solution combustion method at different *F/O*

Nanocatalyst	BET (m^2/g)	P_V (cm^3)	P_d (nm)	Acidity strength		Relative crystallinity[a]		Crystalline size (nm)[b]	
				H_0	(mmol/g)	$CoAl_2O_4$	$S/CoAl_2O_4$	$CoAl_2O_4$	$S/CoAl_2O_4$
$CoAl_2O_4$ (*F/O* = 0.5)	–	–	–	–	–	34.9	–	–	–
$CoAl_2O_4$ (*F/O* = 1)	–	–	–	–	–	100	–	25.2	–
$CoAl_2O_4$ (*F/O* = 1.5)	–	–	–	–	–	88.4	–	24.8	–
$CoAl_2O_4$ (*F/O* = 2)	–	–	–	–	–	67.4	–	23.7	–
$CoAl_2O_4$ (*F/O* = 2.5)	–	–	–	–	–	58.2	–	20.4	–
$S/CoAl_2O_4$ (*F/O* = 0.5)	17.85	0.076	3.3	3.3–0.8	0.323	–	30.3	–	–
$S/CoAl_2O_4$ (*F/O* = 1)	32.60	0.125	4.7	3.3–0.8	0.293	–	100	–	31.6
$S/CoAl_2O_4$ (*F/O* = 1.5)	40.96	0.348	5.6	3.3–0.8	0.340	–	83.3	–	29.3
$S/CoAl_2O_4$ (*F/O* = 2)	32.85	0.102	7.4	3.3–0.8	0.338	–	75.8	–	28.5
$S/CoAl_2O_4$ (*F/O* = 2.5)	29.71	0.101	6.5	3.3–0.8	0.329	–	81.8	–	25.2

[a]Relative crystallinity: XRD relative peak intensity at 2θ = 36.8° for $CoAl_2O_4$ and 25.1° for $S/CoAl_2O_4$

[b]Crystalline size estimated by Scherre's equation at 2θ = 36.8° for $CoAl_2O_4$ and 25.1° for $S/CoAl_2O_4$

crystallinity of spinel $CoAl_2O_4$. Moreover, $S/CoAl_2O_4$ (*F/O* = 0.5) and $S/CoAl_2O_4$ (*F/O* = 1) exhibit transformed structures from amorphous to crystalline form by calcination at 550 °C.

Physicochemical properties of all samples (spinel $CoAl_2O_4$ and its sulfated structure) are tabulated in Table 1. The relative crystallinity decreases by increasing the amount of fuel beyond the stoichiometric ratio

because of the reduction in the growth of crystals of the samples. Crystalline size of the samples approves the described results, implying that S/$CoAl_2O_4$ ($F/O = 1.5$) and S/$CoAl_2O_4$ ($F/O = 2$) exhibit small crystalline size along with single-phase structure ($CoAl_2O_4$).

TG analysis

Plots of TG analysis on $CoAl_2O_4$ samples fabricated at various F/O ratios are presented in Fig. 2. It is well known that results of TG analysis can be used to detect unreacted raw material during a combustion reaction. For this research, the entire sample weight loss range was subdivided into three intervals, namely 50–200 °C, 200–500 °C, and 500–900 °C. The intervals can respectively refer to evaporation of physically adsorbed water on the surface of support [33], pyrolysis of organic groups and/or nitrate precursors [34], and incorporation of cobalt ions in the host material lattice to form $CoAl_2O_4$ or transition of cobalt and alumina from amorphous to crystalline phase [35].

Among other samples, $CoAl_2O_4$ ($F/O = 0.5$) showed the highest weight loss in all of the regions due to less extent of decomposition of nitrate precursors to crystal form during the combustion reaction [31]. On the other hand, less weight loss can observe for the samples fabricated at higher F/O ratio because of higher combustion reaction temperature and duration [33]. The results were in agreement with those of XRD analysis, implying that a higher amount of urea must be used to have the combustion reaction completed. Among others, $CoAl_2O_4$ ($F/O = 2$) shows the smallest weight loss, possibly because of the adoption of the optimum amount of fuel for preparing spinel $CoAl_2O_4$ as support.

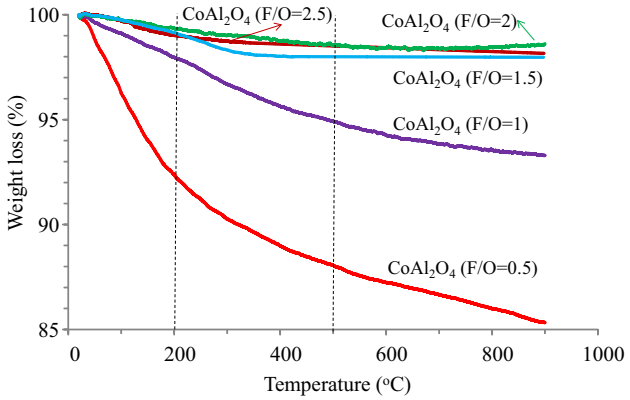

Fig. 2 TG plots of sulfated $CoAl_2O_4$ prepared via solution combustion method at different F/O

FTIR analysis

The FTIR spectra of S/$CoAl_2O_4$ nanocatalysts are depicted in Fig. 3. Plots of all samples exhibit a broad band after 3000 cm^{-1} that is related to O–H vibration of moisture adsorbed on the surface of catalyst as well as a peak at 1640 cm^{-1} [22]. The peak observes at 3550 cm^{-1} for the samples S/$CoAl_2O_4$ ($F/O = 0.5$), and S/$CoAl_2O_4$ ($F/O = 1$) corresponds to OH groups in unreacted raw materials [36]. Al-O bands related to stretching vibrations of AlO_6 and AlO_4

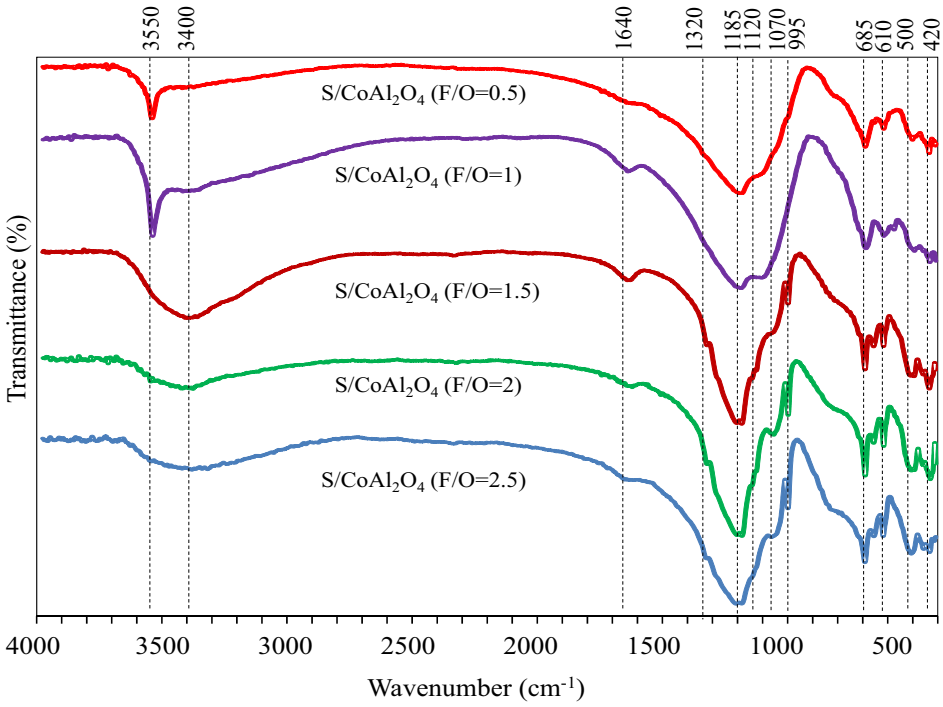

Fig. 3 FTIR spectra of sulfated $CoAl_2O_4$ prepared via solution combustion method at different F/O

structures detect in 500-700 cm^{-1} and 700-850 cm^{-1} bands, respectively [33]. The Co–O vibration peak observes below 500 cm^{-1} [30, 31]. The vibration peaks related to sulfate groups containing S=O and S–O observe in the range of 1000-1400 cm^{-1} [11, 37].

A broad band of sulfate groups observed in S/$CoAl_2O_4$ ($F/O = 0.5$) and S/$CoAl_2O_4$ ($F/O = 1$) spectra becomes narrower by increasing the F/O ratio because of increased availability of metal ions for bonding with sulfate groups. The broad bands could be attributed to the presence of remarkable amounts of free sulfate ions with T_d symmetry on the catalyst surface, resulting in less interaction between sulfate groups and metal ions [15, 38]. On the other hands, symmetric and asymmetric stretching vibrations of S–O band for the samples fabricated at high F/O ratio could detect at 995 cm^{-1} and 1070 cm^{-1}, respectively [39, 40]. The position of sulfate groups peaks can confirm the chelating bidentate form of bonding between SO_4^{2-} and Co-Al oxide surfaces [21, 41].

BET–BJH and acidity analyses

BET results, as listed in Table 1, showed that S/$COAl_2O_4$ ($F/O = 1.5$) has the largest surface area, followed by S/$COAl_2O_4$ ($F/O = 2$). The BET surface area of the samples increased from 17.85 cm^{-1} at F/O ratio of 0.5–40.96 cm^{-1} at F/O ratio of 1.5. The increase could be due to the nourmous amount of exhausted gas and the long combustion time during catalyst preparation [25]. However, a further increase in F/O ratio caused an excessive increase in reaction temperature and time, thereby removing crystals from the support lattice, as seen in XRD analysis results [31]. Although large surface area contributes to higher catalytic activity remarkably but pore diameter plays a significant role in reactions involving reactants with large molecules. In the biodiesel production process, the effect of porosity of catalyst is even more extensive than that of surface area it was reported that pore diameter must be larger than 6 nm to facilitate the permeation of triglycerides macromolecules inside the pores to access available surface area [42]. Among other samples, S/$COAl_2O_4$ ($F/O = 2$) nanocatalysts showed the highest average pore diameter (7.4 nm).

Adsorption–desorption hysteresis curves and pore size distributions of S/$CoAl_2O_4$ nanocatalysts prepared at various F/O ratios are depicted in Fig. 4a. Based on the figure, the samples, except S/$COAl_2O_4$ ($F/O = 0.5$) and S/$COAl_2O_4$ ($F/O = 1.5$), show characteristic curves of type IV material, as per IUPAC classification, which corresponds to mesoporous materials. In addition, their hysteresis cycles approximately are type H3, i.e., related to the plate-like particles that providing slit-shaped pores [10]. The samples prepared at F/O ratio of 0.5 and 1.5 present Type III related to nonporous material in which the pore volume and average pore size data can be referred to voids between the particles. This property can immensely effect on the catalytic activity.

In addition, the pore size distribution of the samples (Fig. 4b) indicates that pore diameter increases with increasing the F/O ratio due to the release of huge volumes of smoke during $CoAl_2O_4$ preparation. In S/$CoAl_2O_4$ ($F/O = 2$) nanocatalyst, the pores in the range of 6–14 nm have a high volume which facilitate the motion of reactant molecules through the porosities.

Based on Table 1, the sample prepared at high F/O ratio (higher than stoichiometric ratio) exhibited higher acidity due to higher crystallinity of the support, thereby contributing to the formation of sulfate-metal ions such as $CoSO_4$ and $Al_2(SO_4)_3$ structures. It is well known that homogeneous mineral acid catalyst such H_2SO_4 is usually used in the esterification reaction. In the esterification reaction, protonation of the carbonyl oxygen by acid makes the carbonyl carbon a much better electrophile and it participates in the making complex with the OH group of an alcohol. Finally, water eliminates and leads to the protonated ester, and the ester is then deprotonated. Note that the acid serves two purposes.

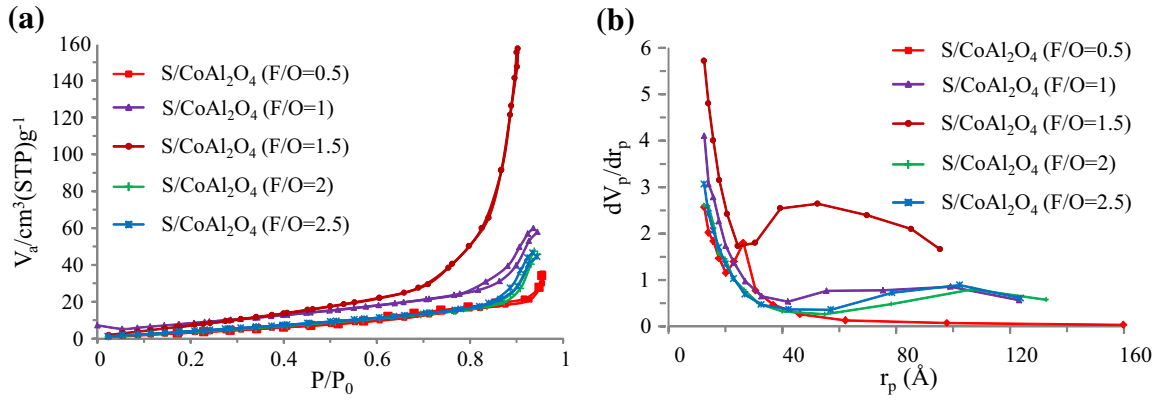

Fig. 4 **a** N_2 adsorption–desorption hysteresis and **b** pore size distribution plots of sulfated $CoAl_2O_4$ prepared via solution combustion method at different F/O

First, it makes the carbonyl carbon a better electrophile and also allows for the loss of H_2O as a leaving group. Therefore, the acidity content of the catalyst is important and directly effects on the activity of a catalyst in the esterification reaction [43].

It must be attended that, although the catalyst with higher acidity presents higher activity, many factors including surface area, pore volume, and crystallinity tends to affect sample activity.

FESEM analysis

FESEM images of S/$CoAl_2O_4$ nanocatalysts prepared by SCM at various *F*/*O* ratios are illustrated in Fig. 5. The sample fabricated at *F*/*O* ratio of 0.5 exhibits an amorphous and agglomerated structure, which is attributed to insufficient combustion reaction temperature and time. By loading more urea as fuel (*F*/*O* = 1), well-shaped particles were formed. However, the resultant structure was denser. Crystal and particle growth continued with increasing the *F*/*O* ratio to up to two, where optimal particle arrangement and diameter were observed. However, higher *F*/*O* ratio (i.e., fuel contents) suppressed the diffusion of oxygen from the air to combustion reaction medium, ending up with incomplete reactions.

EDX analysis

Results of EDX analysis of S/$CoAl_2O_4$ (*F*/*O* = 2) nanocatalyst are shown in Fig. 6a. Accordingly, the sample contains Al, Co, S, and O elements, with no impurity. The S/$CoAl_2O_4$ (*F*/*O* = 2) nanocatalyst shows similar distribution percentages of the elements of Al, Co, and S to those of the

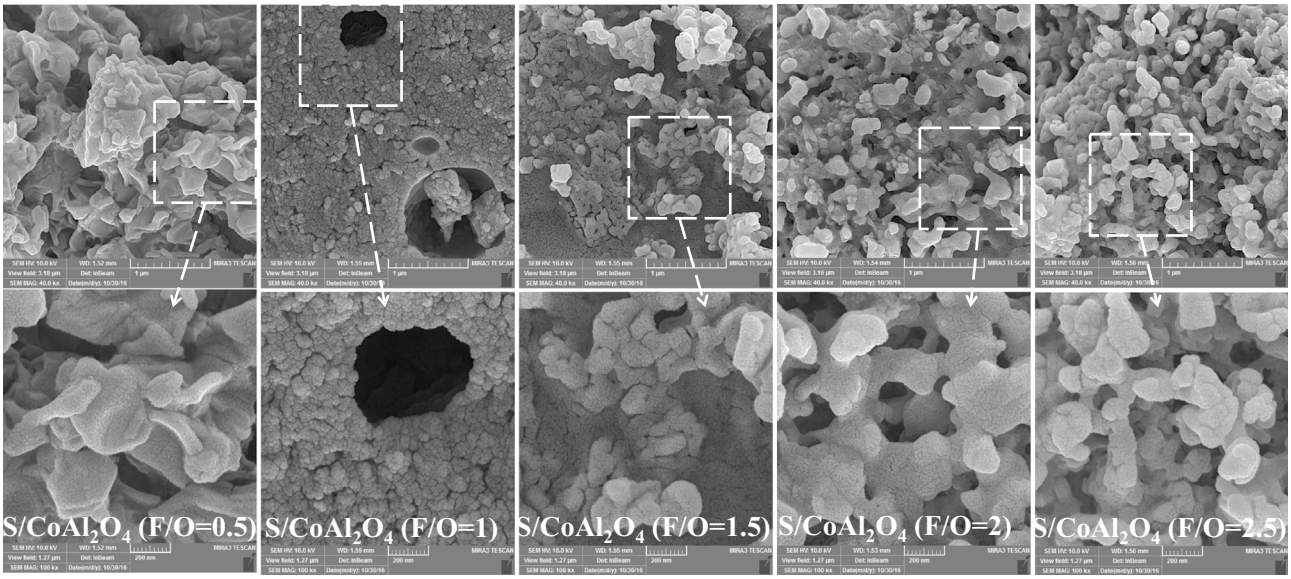

Fig. 5 FESEM images of sulfated $CoAl_2O_4$ nanocatalysts prepared via solution combustion method at different *F*/*O*

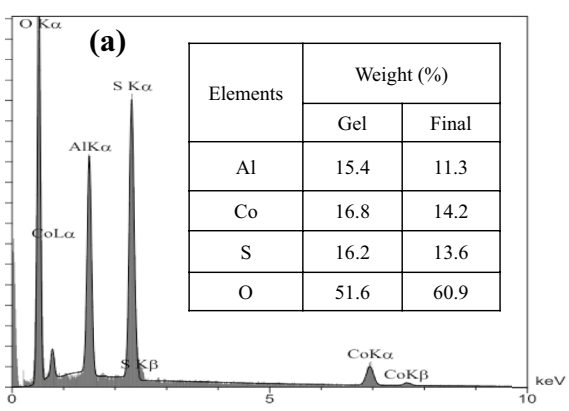

Elements	Weight (%)	
	Gel	Final
Al	15.4	11.3
Co	16.8	14.2
S	16.2	13.6
O	51.6	60.9

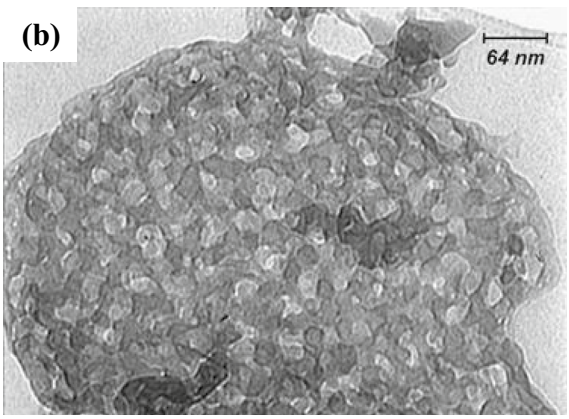

Fig. 6 **a** EDX and **b** TEM images of S/$CoAl_2O_4$ (*F*/*O* = 2) nanocatalyst prepared via solution combustion method

parent solution (15.4%, 16.8%, and 16.2% for Al, Co, and S, respectively). It can confirm well fabrication of nanocatalyst without any loss of nitrate precursors during the combustion reaction.

The TEM image of the nanocatalyst is also presented in Fig. 6b. The particles show a spherical shape with narrower particle size distribution.

The catalytic activity of samples

The activity of the samples in the esterification reaction at MFR of 9 and catalyst amount of 3 wt % was evaluated at two reaction temperatures (90 °C and 120 °C) for the duration of 4 h. The results are presented in Fig. 7. It observes that all of the samples can convert a high amount of oleic acid to its methyl ester at the reaction temperature of 120 °C. It implies high activity of the $CoAl_2O_4$ as support in the esterification reaction, as indicated by superior conversion yields compared to results of similar studies under the same set of conditions [11, 39]. However, to better evaluate the catalytic activity of the samples, the esterification reaction was carried out at a lower reaction temperature (90 °C). As expected, due to the lower reaction rate, lower conversion was obtained. The results reveal that $S/CoAl_2O_4$ ($F/O=2$) nanocatalyst exhibits the highest activity, possibly because of their higher degree of crystallinity, larger pore diameter and surface area, and higher acidity.

Reusability of $S/CoAl_2O_4$ ($F/O=2$) nanocatalyst

The reusability of $S/CoAl_2O_4$ ($F/O=2$) as the optimal nanocatalyst was examined by frequently using the samples in successive runs of esterification reaction. After each run, $S/CoAl_2O_4$ ($F/O=2$) was washed twice with methanol to eliminate unreacted reactants and products from its pores. Then, the sample was dried at 110 °C for 12 h and calcined at 550 °C for 1 h to ensure discharge of porosities. As shown in Fig. 8, the results indicate a reduction the activity of the sample in the second run. It can be related to the gradual removal of sulfate groups with weak bonds from the sample surface as a result of leaching. However, the loss in activity was lower than that reported in some studies on other sulfated catalysts [44]. However, in the next uses, less reduction was observed that can prove the stability of support and well-bonding of sulfate group with support cations. Although the leaching effect was adversely indispensable in this catalyst, regeneration of the catalyst by impregnation with sulfuric acid could improve the results of the reused catalyst.

The activity of the regenerated sample (R-5 in Fig. 8) increased sharply, so that conversion of 96.3% was achieved; i.e., the activity of the sample was comparable to that of the sample in the first use. These results suggest that $S/CoAl_2O_4$ ($F/O=2$) nanocatalyst can be successfully reused at least for four times and simply regenerated for returning its activity, making the nanocatalyst a more environmentally friendly alternative for biodiesel production.

Comparison of the results

The catalyst preparation conditions via this method, along with the activity of the optimum sample in the esterification reactio, was compared and listed in Table 2. Hashemzehi et al. [10] presented that spinel $ZnAl_2O_4$ and $CuAl_2O_4$ fabricated by combustion method had medium activity in the esterification reaction of oleic acid. On the other hands, Wang et al. reported better activity of spinel zinc aluminate by impregnation via the sulfated group. However, they

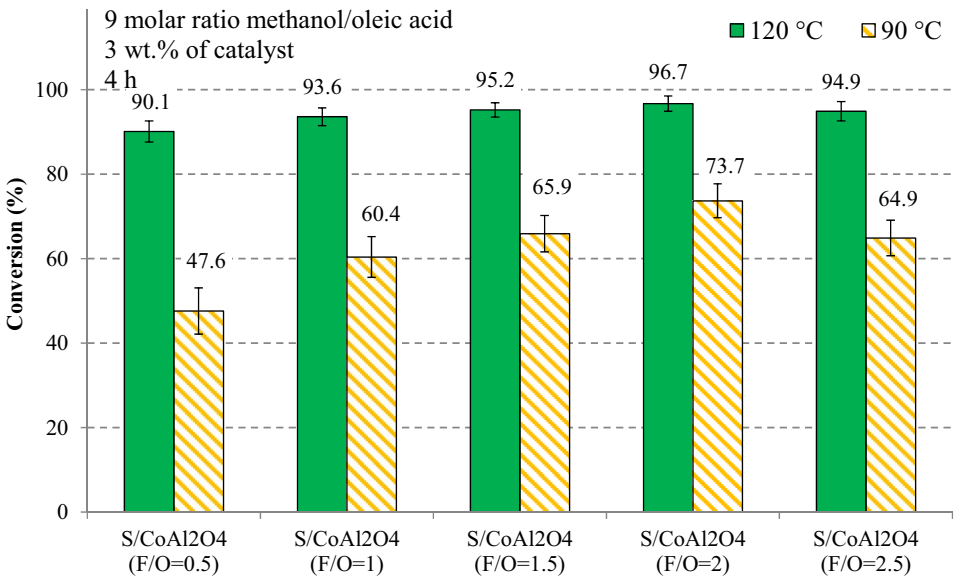

Fig. 7 Activity of sulfated $CoAl_2O_4$ prepared via solution combustion method at different F/O in the esterification reaction

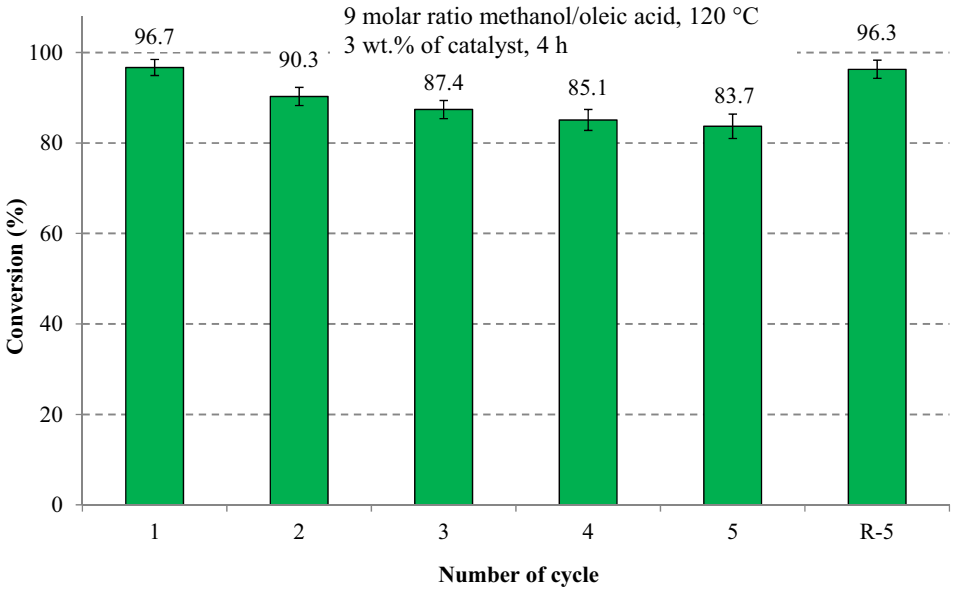

Fig. 8 Reusability of S/$CoAl_2O_4$ ($F/O=2$) nanocatalyst in the esterification reaction

Table 2 Comparison the preparation conditions and catalytic activity of the S/$CoAl_2O_4$ ($F/O=2$) with other catalysts in the esterification reaction

Catalyst	Catalyst preparation conditions			Esterification reaction conditions					References
	PM	Pt	CTP (°C)	RT	CA	MFR	Rt	Y	
$SO_4^{2-}/CoAl_2O_4$	Combustion-impregnation	5	550	120	3	9	4	96.7	This study
$SO_4^{2-}/ZnAl_2O_4$	Sol gel-impregnating	30	600	65	5	25	8	70	[21]
$Ni/ZnAl_2O_4$	Hydrothermal	20	450	280	2.5	20	6	50	[45]
$CuAl_2O_4$	Combustion	2	–	180	3	9	6	94	[10]
Aluminosilicate	Impregnation	10	120	150	3	6	9	89	[8]
$SO_4^{2-}/La^{3+}/C$	Impregnation	20	400	62	0.75	9	5	98.4	[9]
SO_4^{2-}/Fe_3O_4	Impregnation	30	500	105	10	1	4	68	[46]
Mg/Al	Coprecipitation	20	500	110	3	6	6	66.1	[47]

PM Preparation method, *Pt* preparation time, *PCT* calcination temperature of preparation, *RT* reaction temperature, *CA* catalyst amount, *MOR* methanol-FFA molar ratio, *Rt* reaction time, *Y* yield

used more time for fabrication the catalyst. $Ni/ZnAl_2O_4$ also showed less activity even at the reaction temperature of 280 °C [45]. The results of other researches also exhibit that the combustion method requires less time for fabrication of the final powder and the prepared nanocatalyst has high activity in the esterification reaction due to its appropriate properties.

Conclusion

Synthesis active, stable, and less-corrosive heterogeneous catalyst is recently concerned for production of biodiesel during esterification and transesterification reaction. For this purpose, $CoAl_2O_4$ spinel was firstly synthesized via SCM and impregnated by sulfate groups to prepare a catalyst for esterification reaction. Amount of urea as fuel in the $CoAl_2O_4$ spinel preparation process was optimized by assessing its influence on structure and performance of the support and sulfated nanocatalyst. The results indicated that S/$CoAl_2O_4$ ($F/O=2$) nanocatalyst had the highest level of activity as a result of its large surface area, a high degree of crystallinity, large pore diameter, and small crystalline size. It converted 96.7% of oleic acid (as FFA) to biodiesel at middle esterification reaction conditions. Comparing the performance of the S/$CoAl_2O_4$ ($F/O=2$) nanocatalyst to other catalysts studied in related literature confirms the high activity of the sample along with its straightforward and cost and energy effective synthesis procedure. Furthermore, it could be easily regenerated without any loss of activity, confirming enormous potentials of $CoAl_2O_4$ as a support for similar chemical reactions due to its mechanical and chemical resistance properties.

Acknowledgements We would like to show our gratitude to the Ferdowsi University of Mashhad for the financial support of the research (Grant number: 32009) and patial finantial supporting of Iran Nanotechnology Initiative Council (Grant number: 121638).

Author contribution Mr. Azmoon and Mr. Heydari performed the experiments. They also had written the manuscript. Dr. Nayebzadeh and Dr. Saghatoleslami checked the manuscript English level and quality of the experiment and the results as a supervisor and advisor, respectively. They also analyzed the characterization results.

References

1. Chuah, L.F., Klemeš, J.J., Yusup, S., Bokhari, A., Akbar, M.M.: A review of cleaner intensification technologies in biodiesel production. J. Clean. Prod. **146**, 181–193 (2017)
2. Soltani, S., Rashid, U., Al-Resayes, S.I., Nehdi, I.A.: Recent progress in synthesis and surface functionalization of mesoporous acidic heterogeneous catalysts for esterification of free fatty acid feedstocks: a review. Energy Convers. Manag. **141**, 183–205 (2017)
3. Mahmudul, H.M., Hagos, F.Y., Mamat, R., Adam, A.A., Ishak, W.F.W., Alenezi, R.: Production, characterization and performance of biodiesel as an alternative fuel in diesel engines—a review. Renew. Sustain. Energy Rev. **72**, 497–509 (2017)
4. Shokuhi Rad, A., Hoseini Nia, M., Ardestani, F., Nayebzadeh, H.: Esterification of waste chicken fat: sulfonated MWCNT toward biodiesel production. Waste Biomass Valoriz. **9**, 591–599 (2016)
5. Nayebzadeh, H., Saghatoleslami, N., Haghighi, M., Tabasizadeh, M.: Influence of fuel type on microwave-enhanced fabrication of KOH/$Ca_{12}Al_{14}O_{33}$ nanocatalyst for biodiesel production via microwave heating. J. Taiwan Inst. Chem. Eng. **75**, 148–155 (2017)
6. Mardhiah, H.H., Ong, H.C., Masjuki, H.H., Lim, S., Lee, H.V.: A review on latest developments and future prospects of heterogeneous catalyst in biodiesel production from non-edible oils. Renew. Sustain. Energy Rev. **67**, 1225–1236 (2017)
7. Dai, Y.-M., Lin, J.-H., Chen, H.-C., Chen, C.-C.: Potential of using ceramics wastes as a solid catalyst in biodiesel production. J. Taiwan Inst. Chem. Eng. **91**, 427–433 (2018)
8. Phukan, A., Bhorodwaj, S.K., Sharma, P.P., Dutta, D.K.: Mesoporous aluminosilicate: efficient and reusable catalysts for esterification of sec-butanol with acetic acid. J. Porous Mater. **25**(1), 129–136 (2018)
9. Shu, Q., Tang, G., Lesmana, H., Zou, L., Xiong, D.: Preparation, characterization and application of a novel solid Brönsted acid catalyst SO_4^{2-}/La^{3+}/C for biodiesel production via esterification of oleic acid and methanol. Renew. Energy **119**, 253–261 (2018)
10. Hashemzehi, M., Saghatoleslami, N., Nayebzadeh, H.: Microwave-assisted solution combustion synthesis of spinel-type mixed oxides for esterification reaction. Chem. Eng. Commun. **204**(4), 415–423 (2016)
11. Duan, Y., Wu, Y., Shi, Y., Yang, M., Zhang, Q., Hu, H.: Esterification of octanoic acid using SiO_2 doped sulfated aluminum-based solid acid as catalyst. Catal. Commun. **82**, 32–35 (2016)
12. Wang, C., Gui, X., Yun, Z.: Esterification of lauric and oleic acids with methanol over oxidized and sulfonated activated carbon catalyst. React. Kinet. Mech. Catal. **113**(1), 211–223 (2014)
13. Kuzminska, M., Backov, R., Gaigneaux, E.M.: Complementarity of heterogeneous and homogeneous catalysis for oleic acid esterification with trimethylolpropane over ion-exchange resins. Catal. Commun. **59**, 222–225 (2015)
14. Wahidin, S., Idris, A., Shaleh, S.R.M.: Ionic liquid as a promising biobased green solvent in combination with microwave irradiation for direct biodiesel production. Bioresour. Technol. **206**, 150–154 (2016)
15. Saravanan, K., Tyagi, B., Shukla, R.S., Bajaj, H.C.: Solvent free synthesis of methyl palmitate over sulfated zirconia solid acid catalyst. Fuel **165**, 298–305 (2016)
16. Saravanan, K., Tyagi, B., Bajaj, H.C.: Nano-crystalline, mesoporous aerogel sulfated zirconia as an efficient catalyst for esterification of stearic acid with methanol. Appl. Catal. B **192**, 161–170 (2016)
17. Gopinath, S., Kumar, P.S.M., Arafath, K.A.Y., Thiruvengadaravi, K.V., Sivanesan, S., Baskaralingam, P.: Efficient mesoporous SO_4^{2-}/Zr-KIT-6 solid acid catalyst for green diesel production from esterification of oleic acid. Fuel **203**, 488–500 (2017)
18. Nayebzadeh, H., Haghighi, M., Saghatoleslami, N., Tabasizadeh, M., Yousefi, S.: Fabrication of carbonated alumina doped by calcium oxide via microwave combustion method used as nanocatalyst in biodiesel production: influence of carbon source type. Energy Convers. Manag. **171**, 566–575 (2018)
19. Nayebzadeh, H., Saghatoleslami, N., Haghighi, M., Tabasizadeh, M., Binaeian, E.: Comparative assessment of the ability of a microwave absorber nanocatalyst in the microwave-assisted biodiesel production process. Compt. Rendus Chim. **21**(7), 676–683 (2018)
20. Smoláková, L., Pöpperle, L., KocíkLada, J., Horáček, D., Čapek, L.: Catalytic behavior of Mg–Al and Zn–Al mixed oxides in the transesterification of rapeseed oil: comparison of batch and fixed bed reactors. React. Kinet. Mech. Catal. **121**(1), 209–224 (2017)
21. Wang, A., Wang, J., Lu, C., Xu, M., Lv, J., Wu, X.: Esterification for biofuel synthesis over an eco-friendly and efficient kaolinite-supported $SO_4^{2-}/ZnAl_2O_4$ macroporous solid acid catalyst. Fuel **234**, 430–440 (2018)
22. Hashemzehi, M., Saghatoleslami, N., Nayebzadeh, H.: A study on the structure and catalytic performance of $Zn_xCu_{1-x}Al_2O_4$ catalysts synthesized by the solution combustion method for the esterification reaction. Comptes Rendus Chim. **19**(8), 955–962 (2016)
23. Soltani, S., Rashid, U., ArbiNehdib, I., Al-Resayes, S.I., Al-Muhtaseb, A.A.H.: Sulfonated mesoporous zinc aluminate catalyst for biodiesel production from high free fatty acid feedstock using microwave heating system. J. Taiwan Inst. Chem. Eng. **70**, 219–228 (2017)
24. Rahmani Vahid, B., Haghighi, M.: Biodiesel production from sunflower oil over MgO/$MgAl_2O_4$ nanocatalyst: effect of fuel type on catalyst nanostructure and performance. Energy Convers. Manag. **134**, 290–300 (2017)
25. Nayebzadeh, H., Saghatoleslami, N., Tabasizadeh, M.: Application of microwave irradiation for preparation of a KOH/calcium aluminate nanocatalyst and biodiesel. Chem. Eng. Technol. **40**(10), 1826–1834 (2017)
26. Podbolotov, K.B., Khort, A.A., Tarasov, A.B., Trusov, G.V., Roslyakov, S.I., Mukasyan, A.S.: Solution Combustion synthesis of copper nanopowders: the fuel effect. Combust. Sci. Technol. **189**(11), 1878–1890 (2017)
27. Sudheesh, V.D., Thomas, N., Roona, N., Baghya, P.K., Sebastian, V.: Synthesis, characterization and influence of fuel to oxidizer ratio on the properties of spinel ferrite (MFe2O4, M = Co and

Ni) prepared by solution combustion method. Ceram. Int. **43**(17), 15002–15009 (2017)
28. Topaloğlu Yazıcı, D., Bilgiç, C.: Determining the surface acidic properties of solid catalysts by amine titration using Hammett indicators and FTIR-pyridine adsorption methods. Surf. Interface Anal. **42**(6–7), 959–962 (2010)
29. Rahmani Vahid, B., Haghighi, M.: Urea-nitrate combustion synthesis of $MgO/MgAl_2O_4$ nanocatalyst used in biodiesel production from sunflower oil: influence of fuel ratio on catalytic properties and performance. Energy Convers. Manag. **126**, 362–372 (2016)
30. Reynoso, A.J., Ayastuy, J.L., Iriarte-Velasco, U., Gutiérrez-Ortiz, M.A.: Cobalt aluminate spinel-derived catalysts for glycerol aqueous phase reforming. Appl. Catal. B **239**, 86–101 (2018)
31. Pourgolmohammad, B., Masoudpanah, S.M., Aboutalebi, M.R.: Synthesis of $CoFe_2O_4$ powders with high surface area by solution combustion method: effect of fuel content and cobalt precursor. Ceram. Int. **43**(4), 3797–3803 (2017)
32. Khoshbin, R., Haghighi, M., Margan, P.: Combustion dispersion of $CuO–ZnO–Al_2O_3$ nanocatalyst over HZSM-5 used in DME production as a green fuel: effect of citric acid to nitrate ratio on catalyst properties and performance. Energy Convers. Manag. **120**, 1–12 (2016)
33. Nayebzadeh, H., Haghighi, M., Saghatoleslami, N., Alaei, S., Yousefi, S.: Texture/phase evolution during plasma treatment of microwave-combustion synthesized $KOH/Ca_{12}Al_{14}O_{33}$-C nanocatalyst for reusability enhancement in conversion of canola oil to biodiesel. Renew. Energy **139**, 28–39 (2019)
34. Kumar, P., Srivastava, V.C., Mishra, I.M.: Dimethyl carbonate synthesis via transesterification of propylene carbonate with methanol by ceria-zinc catalysts: role of catalyst support and reaction parameters. Korean J. Chem. Eng. **32**(9), 1774–1783 (2015)
35. Ita, B.I., Magu, T.O., Ehi-Eromosele, C.O.: Physico-Chemical Properties of Biodiesel Obtained from Jatropha Curcas Seeds Oil Using CoMgFe2O4 and MgFe2O4 as Nanocatalysts. J. Ind. Technol. **3**(1), 1–16 (2018)
36. Nayebzadeh, H., Saghatoleslami, N., Tabasizadeh, M.: Application of microwave irradiation for fabrication of sulfated $ZrO_2–Al_2O_3$ nanocomposite via combustion method for esterification reaction: process condition evaluation. J. Nanostruct. Chem. **9**(2), 141–152 (2019)
37. Rahmani Vahid, B., Saghatoleslami, N., Nayebzadeh, H., Toghiani, J.: Effect of alumina loading on the properties and activity of SO_4^{2-}/ZrO_2 for biodiesel production: process optimization via response surface methodology. J. Taiwan Inst. Chem. Eng. **83**, 115–123 (2018)
38. Kaur, K., Wanchoo, R.K., Toor, A.P.: Sulfated iron oxide: a proficient catalyst for esterification of butanoic acid with glycerol. Ind. Eng. Chem. Res. **54**(13), 3285–3292 (2015)
39. Huang, C.-C., Yang, C.-J., Gao, P.-J., Wang, N.-C., Chen, C.-L., Chang, J.-S.: Characterization of an alkaline earth metal-doped solid superacid and its activity for the esterification of oleic acid with methanol. Green Chem. **17**(6), 3609–3620 (2015)
40. Setayesh, S.R., Abolhasani, E., Ghasemi, S.: Characterisation of nanocrystalline sulfated titania modified with transition metals and aluminum as solid acids for esterification. Prog. React. Kinet. Mech. **41**(1), 57–66 (2016)
41. Gardy, J., Osatiashtiani, A., Céspedes, O., Hassanpour, A., Lai, X., Lee, A.F., Wilson, K., Rehan, M.: A magnetically separable $SO_4/Fe\text{-}Al\text{-}TiO_2$ solid acid catalyst for biodiesel production from waste cooking oil. Appl. Catal. B **234**, 268–278 (2018)
42. Hojjat, M., Nayebzadeh, H., Khadangi-Mahrood, M., Rahmani-Vahid, B.: Optimization of process conditions for biodiesel production over $CaO–Al_2O_3/ZrO_2$ catalyst using response surface methodology. Chem. Pap. **71**(3), 689–698 (2016)
43. Murad, P.C., Hamerski, F., Corazza, M.L., Luz, L.F.L., Voll, F.A.P.: Acid-catalyzed esterification of free fatty acids with ethanol: an assessment of acid oil pretreatment, kinetic modeling and simulation. React. Kinet. Mech. Catal. **123**(2), 505–515 (2018)
44. Shao, G.N., Sheikh, R., Hilonga, A., Lee, J.E., Park, Y.-H., Kim, H.T.: Biodiesel production by sulfated mesoporous titania–silica catalysts synthesized by the sol–gel process from less expensive precursors. Chem. Eng. J. **215–216**, 600–607 (2013)
45. Li, G., Chen, L., Fan, R., Liu, D., Chen, S., Li, X., Chung, K.H.: Catalytic deoxygenation of C18 fatty acid over supported metal Ni catalysts promoted by the basic sites of $ZnAl_2O_4$ spinel phase. Catal. Sci. Technol. **9**(1), 213–222 (2019)
46. Kaur, J., Kaur, K., Toor, A.P.: Sulfated iron oxide-catalyzed esterification of acetic acid with n-butanol by reactive distillation. Chem. Eng. Technol. **41**(11), 2196–2202 (2018)
47. Kuljiraseth, J., Wangriya, A., Malones, J.M.C., Klysubun, W., Jitkarnka, S.: Synthesis and characterization of AMO LDH-derived mixed oxides with various Mg/Al ratios as acid–basic catalysts for esterification of benzoic acid with 2-ethylhexanol. Appl. Catal. B **243**, 415–427 (2019)